Innovative 3-D Printing Processing Techniques for Flexible and Wearable Planar Rectennas

Innovative 3-D Printing Processing Techniques for Flexible and Wearable Planar Rectennas

Giulia Battistini
DEI "Guglielmo Marconi"
University of Bologna
Bologna, Italy
giulia.battistini8@studio.unibo.it

Giacomo Paolini
DEI "Guglielmo Marconi"
University of Bologna
Bologna, Italy
giacomo.paolini4@unibo.it

Diego Masotti
DEI "Guglielmo Marconi"
University of Bologna
Bologna, Italy
diego.masotti@unibo.it

Alessandra Costanzo
DEI "Guglielmo Marconi"
University of Bologna
Bologna, Italy
alessandra.costanzo@unibo.it

***Abstract*—This work demonstrates the use of a low-cost, lossy, flexible substrate processed by novel 3-D printing techniques which significantly mitigate its intrinsic losses, thus providing performance comparable to those of traditional substrates. These processing techniques are applied to both microstrip and coplanar waveguide structures; they are first derived theoretically, starting from the electromagnetic theory of modes propagation, then numerically validated by full-wave analysis, and finally experimentally verified. The design of a miniaturized 868 MHz rectenna, adopting a coplanar-fed patch antenna based on the proposed fabrication approach, is presented. By means of nonlinear/electromagnetic co-design, the antenna is directly matched to the rectifier. A 30-dB power range starting from –20 dBm is considered. Direct matching allows to get rid of a dedicated matching network and its associated losses, resulting in a slight efficiency increase and a significant reduction of the overall dimensions. Finally, the 3-D-printed prototype is presented: the overall rectenna performance proves that design freedom enabled by 3-D printing paves the way to the use of low-cost flexible dielectric materials, even with poor electromagnetic properties, to realize wearable battery-free wireless nodes.**

Keywords—3-D printing, conjugate matching, coplanar patch antenna, flexible, rectifier, wearable electronics.

I. Introduction

In the latest years, many solutions exploiting wireless power transfer (WPT) and energy harvesting (EH) technologies have been addressed to many fields of interest; the aim is to get advantage from these techniques in order to eliminate bulky batteries and the need for their maintenance.

In particular, for what concerns medical sciences and biomedical engineering, daily continuous health monitoring of elderly and impaired people could be performed with the employment of implantable and/or wearable sensing devices. In this fields of applications, non-conventional materials are worthy to be used as substrates or as encapsulating materials such as polymers, namely parylene, polyimide (PI), polydimethylsiloxane (PDMS), because of their bio-compatibility, extensibility, extreme flexibility, and long-term stability, also in corrosive environments [1].

In this work, a 3-D printable flexible resin material has been chosen as the substrate for the design of a wearable 868 MHz rectenna for WPT applications. For these purposes, shielded planar technologies, such as the grounded coplanar waveguide (GCPW) one, have been selected to decouple their performance from the presence of body tissues. The chosen material has been characterized from the electromagnetic (EM) point of view, through resonant techniques similar to those adopted in [2] and [3], and resulted to be a highly lossy medium. Thus, drawing inspiration from pioneering micromachining techniques such those presented in [4], different new approaches have been investigated in order to reduce the impact of its losses in terms of both propagation and radiation performances. In particular, for the antenna-rectifier subsystem, GCPW has been selected, and different types of dielectric etchings have been investigated with the twofold goal of minimizing the electric field propagation through the lossy material and ensuring mechanical stability of the whole system. Techniques similar to [5] and [6] have been adopted for the antenna subsystem, where a large portion of its substrate has been subtracted, leaving thin layers at the top and bottom of the structure to support the adhesive metallization.

Although materials, as thin as a 0.18 mm, have been reported in the literature as the substrate for a flexible monopole [7] and a meshed antenna on Kapton [8], a 2-mm substrate has been chosen for the present project to adopt a patch-like antenna for flexibility and wearability purposes, thanks to the presence of a ground plane.

Finally, for the connection of the antenna with the rectifying circuit, the matching network is removed, and the conjugate matching technique is applied, as described in [9] and [10], with the aim of reducing the overall dimensions of the circuitry parts, thus minimizing the dielectric losses. The flexible rectenna results in terms of overall power conversion efficiency are appreciable and comparable to those achieved using traditional substrates.

II. Miniaturized Coplanar-Fed Patch Antenna Design on Flexible 80A

A. 3-D Printing Techniques to Improve Propagation in Lossy Substrates

The material Flexible 80A is a low-cost resin 3-D printable material distributed by Formlabs (Somerville, MA, USA). Moreover, this material can be treated to be flexible; in particular, post-curing for Flexible 80A previews its heating at 60°C for ten minutes, guaranteeing a tensile strength of +140%. To the authors' knowledge this material has not been used before as a substrate for microwave circuits and its electromagnetic characteristics are not available in any

frequency band. Thus, the first activity to be carried out is to uniquely establish the loss tangent ($tan(\delta)$) and permittivity (ε_r) of a 2 mm-thick material sample: Flexible 80A has been characterized by means of the T-resonator method, up to 6 GHz, to include higher harmonics characterization in view of its use for the nonlinear design of the rectenna. In particular, at the antenna operating frequency of 868 MHz, $\varepsilon_r = 2.7$ and $tan(\delta) = 0.11$ are the extracted values, from which the conductivity $\sigma = 2.34 \cdot 10^{-3}$ has been obtained. Since the substrate resulted to be quite lossy, innovative techniques have been investigated to improve the propagation and radiation performance.

To begin with, as expected, it has been demonstrated that the GCPW technology reduces the losses with respect to the microstrip one. In fact, in GCPW the field is mainly concentrated in the region around the gaps between the hot line and the coplanar grounds on top of the substrate, which means that, with respect to the microstrip, the field propagates mostly in the air and the amount of field penetrating the lossy material is reduced. Moreover, the design freedom provided by 3-D printing, allowed to suitably customize the region where most of the electric field density is located, thus modifying the effective EM properties of the material.

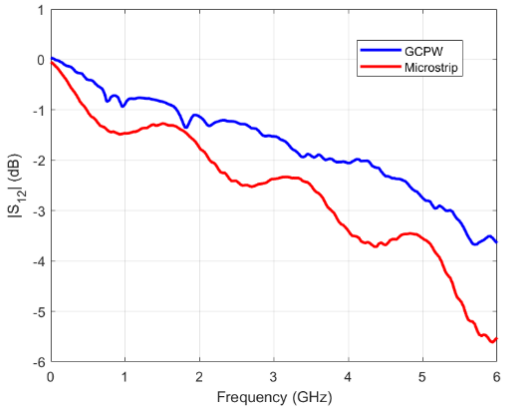

Fig. 1. Comparison between $|S_{12}|$ curves of a measured microstrip line and a GCPW realized with copper tape on a sample of Flexible 80A substrate.

Therefore, in this work the substrate has been dug in the gaps among the hot and ground coplanar conductors with the goal of allowing the majority of the quasi-transverse electromagnetic (quasi-TEM) electric field being located in the air, thus reducing the losses due to the propagation in the lossy material. Fig. 1 shows the broadband transmission coefficient behavior of two 50-Ω transmission lines samples with same length of 100 mm, realized on the Flexible 80A in microstrip and GCPW technologies, respectively; it is possible to notice that, at the operating frequency of interest, the microstrip line introduces a 0.6-dB attenuation higher than the GCPW, while at the highest measured frequency (6 GHz) this difference exceeds 2 dB.

Thus, the GCPW technology has been selected for the present project and different 3-D printed etches have been studied, with the goal described above. As a representative example, Fig. 2 shows the comparison between the measured and simulated magnitude of the $|S_{12}|$ parameters of two GCPW realizations, one without etching the gaps, the other with rectangular-shape etchings (see Figs. 3). Both simulations and measurements demonstrate that the rectangular excavations provide great benefits reducing the losses especially at higher frequencies, paving the way for future exploitation of this 3-D printing solution at higher operating frequencies.

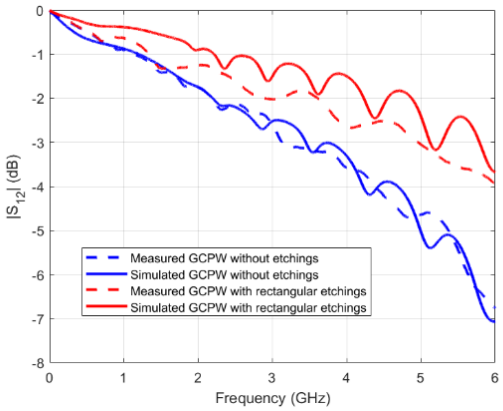

Fig. 2. Comparison between the measured and simulated $|S_{12}|$ curves of the GCPWs with and without substrate rectangular etchings.

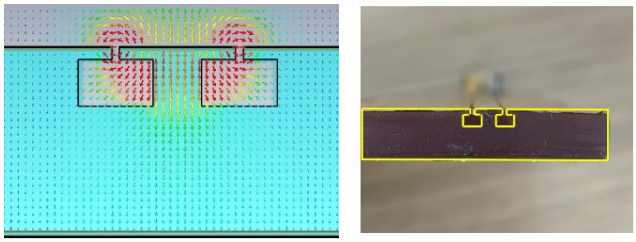

(a) (b)

Fig. 3. (a) CST layout and (b) prototype of the GCPW realized with rectangular etchings.

B. Shrinked Coplanar-Fed Patch Antenna Design on Flexible 80A

A coplanar-fed patch antenna has been firstly designed at 868 MHz on the abovementioned resin substrate, and further excavation techniques have been exploited to improve the antenna radiation performance on such a lossy substrate.

In order to miniaturize the antenna, a shorting plate of copper has been used to connect the top side of the patch to its ground plane placed at the bottom of the structure. This technique allows to significantly reduce the patch length (about 50%), and a value of 55-mm length has been obtained. Since the coplanar waveguide width and gaps have been dimensioned to obtain a 50-Ω characteristic line impedance, the patch width has been optimized in such a way to achieve the impedance matching to its feeding line.

As discussed above, 3-D printing, and substrate etching in particular, allows to obtain better effective dielectric characteristics, that are reduced effective dielectric constant and loss tangent. Therefore, the substrate has been machined by removing cubes with a 4-mm side and spaced by 2 mm, leaving a 500-μm layer at the top and bottom of the substrate, for attaching the adhesive metal layers (see Fig. 4). Moreover, 0.5 mm-deep etchings have been realized in correspondence of the waveguide feeding line gaps to reduce the propagation losses, as explained in the previous section.

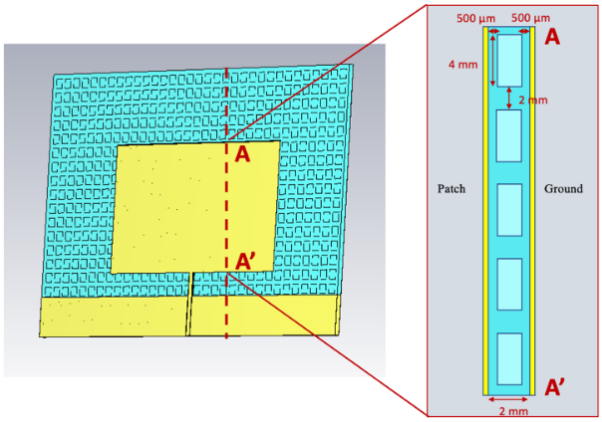

Fig. 4. Layout of the designed coplanar patch antenna, with a callout on the weft of the trasversal section of the substrate.

The resulting antenna structure has been simulated on CST Microwave Studio and the obtained results show that the antenna performance benefits from both these fabrication choices solutions, leading to a realized gain of –3.14 dBi at the frequency of 868 MHz and a radiation efficiency of 14.9%. These performances are acceptable, considering the choice of using a layer extremely thin for an 868 MHz patch antenna, and are doubled with respect to those predicted without customized etching, being 6.3% and –6 dBi, respectively. Furthermore, simulations have confirmed that, by relaxing the constraint on the substrate thinness, the performance improve accordingly. For example, using a 1-cm thick Flexible 80A, suitably etched, the radiation efficiency rises to 59%, but in this case the prototype would lose its flexibility.

III. Rectifier Design and Rectenna Performance

Especially at high frequency, where distributed topologies are recommended, the design of the impedance matching network may increase cost, footprint, and losses. Since this work aim is to overcome the intrinsic losses caused by the dielectric substrate, here we propose the design comparisons between two rectennas (with two almost equally efficient antennas): one adopting a hybrid matching network (with the distributed components realized in GCPW technology and one lumped component) between the antenna and the rectifier, and the other one realizing a direct conjugate matching, by varying the antenna input port impedance. The same rectifier topology is chosen consisting of a voltage-doubler (using two Skyworks SMS7630-079LF Schottky diodes). These two rectennas have been designed and simulated by means of the harmonic balance simulation on Keysight ADS. The optimum load for both cases is about 890 Ω.

The rectenna layouts schematics are shown in Figs. 5 (a) and (b), respectively, whereas Fig. 5 (c) shows the final prototype realization of the conjugate-matched solution. In Fig. 5 (a), between the antenna and the rectifier, a matching network in GCPW technology is shown. The choice of using GCPW is compliant with the study presented in Section II, and adopts the etching technique of the substrate under the gaps, to reduce the dielectric losses. The external matching network has been realized with an input capacitor (C_{MN} = 23.3 pF), two 50-Ω open stubs in GPCW technology (length: 15.33 mm each), and a meandered 50-Ω grounded coplanar waveguide (total length: 63.27 mm).

In Fig. 5 (b), the direct connection is schematically depicted; in order to eliminate the matching network, the antenna has been modified in such a way to show an impedance that is as much as possible the conjugate-matched of the rectifier input impedance, for a selected rectifier input power range. This step is not straightforward due to the fact that the rectifier is a nonlinear circuit, thus, the input impedance not only varies with frequency, but also input power must be accounted for in the nonlinear/EM co-design process.

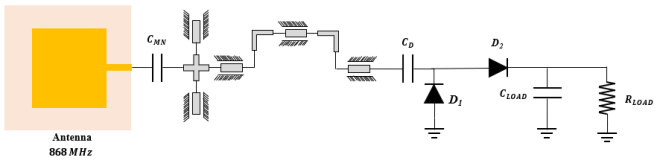

(a)

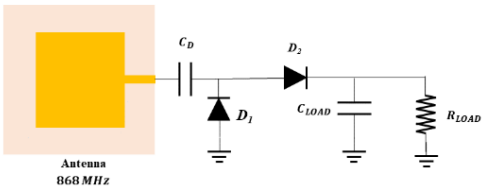

(b)

(c)

Fig. 5. Schematic of the (a) rectenna with an external GCPW matching network, and (b) the rectenna realized through the conjugate matching technique. (c) Picture of the realized prototype of the antenna with copper tape on Flexible 80A.

Therefore, an accurate nonlinear analysis of the rectifier input impedance variation at the rectenna operating frequency of 868 MHz, accounting for eight harmonics, has been carried out over the radiofrequency (RF) power range spanning from –20 to 10 dBm. In Fig. 6, the real and imaginary components of the rectifier input impedance are plotted versus the RF power received by the antenna (P_{av}), simulated as a power source generator. It can be observed that they vary significantly: the real part in the interval [76 ÷ 143] Ω, the imaginary one in the interval [–282 ÷ –32] Ω. Thus, a trade-off value for the antenna impedance has been chosen equal to Z_A = 165.35 + j36.4. This result has been achieved by varying the antenna width (final value: 110 mm), instead of creating insets on its metallization that could be difficult to realize with the chosen adhesive copper (due to out-of-control accuracy of the cutting procedure).

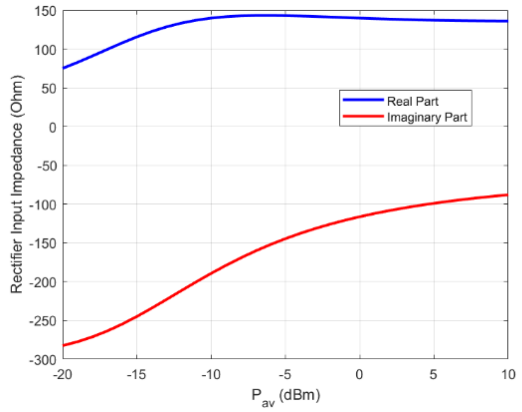

Fig. 6. Simulated rectifier input impedance versus total received input power.

Fig. 7 (a) shows the comparison between the simulated results of the two rectenna projects, in terms of RF-to-dc efficiency as a function of the RF power entering the rectifiers (P_{in}), that is accounting for the (poor) antenna radiation efficiency resulting from its EM simulation; such reduced quantity must be considered to accurately quantify the power truly entering the rectifier [11] and is estimated starting from the effective antenna radiation efficiency. P_{in} versus P_{av} is plotted in Fig. 7 (b) and the corresponding predicted rectenna dc output power is also shown.

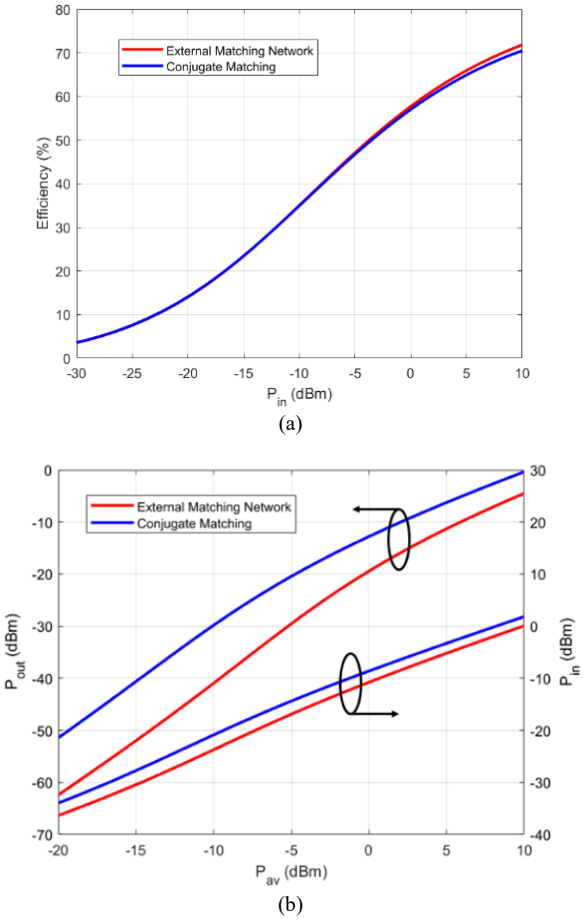

Fig. 7. (a) Rectifier power conversion efficiency versus power actually entering the rectifier (P_{in}); (b) dc output power (P_{out}) and P_{in} versus available power (P_{av}), with and without matching network.

It can be concluded that for both the rectenna projects, the rectifier has the same efficiency, as expected, reaching a maximum of 70% with P_{in} = 10 dBm. However, due to the reduced antenna radiation efficiency, about 14.9%, the effective rectenna efficiency results to be lower, in accordance with the theory of [11]. Plots of Fig. 7 (b) clearly demonstrate that the conjugated-matched rectenna outperforms the standard one with respect to both the dc output power and the overall dimensions.

IV. Conclusion

This work has been dedicated to investigate the exploitation of flexible and low-cost materials for their utilization as substrates for realizing wearable RF circuits and systems. In particular, the design of an 868 MHz rectenna has been presented using a 2-mm thick Flexible 80A substrate suitable etched by means of 3-D printing techniques. The exploitation of innovative etching techniques to minimize the dielectric losses have been theoretically and numerically studied for both the feeding network and the antenna subsystems adopting the GCPW technology. These procedures lead to double the realized gain of the antenna with respect to the counterpart realized in microstrip technology. Finally, the antenna is connected to a voltage-doubler rectifier by means of a hybrid matching network and by getting rid of it taking advantage of the conjugate matching technique. The latter shows a twofold improvement both in terms of the total RF-to-dc power conversion efficiency and of the reduced circuit footprint.

References

[1] C. Hassler, T. Boretius, and T. Stieglitz, “Polymers for neural implants”, Journal of Polymer Science Part B: Polymer Physics, vol. 49, no. 1, pp. 18-33, 2011.

[2] V. Rizzoli, “Resonance Measurement of Single- and Coupled-Microstrip Propagation Constants,” IEEE Trans. Microw. Theory Techn., vol. 25, no. 2, pp. 113-120, February 1977.

[3] K.-P. Latti, M. Kettunen, J. Strom, and P. Silventoinen, “A Review of Microstrip T-Resonator Method in Determining the Dielectric Properties of Printed Circuit Board Materials,” IEEE Trans. Instrum. Meas., vol. 56, no. 5, pp. 1845-1850, October 2007.

[4] K. J. Herrick, T. A. Schwarz, and L. P. B. Katehi, “Si-micromachined coplanar waveguides for use in high-frequency circuits,” IEEE Trans. Microw. Theory Techn., vol. 46, no. 6, pp. 762-768, June 1998.

[5] Y. Kim and S. Lim, “Low Loss Substrate-Integrated Waveguide Using 3D-Printed Non-Uniform Honeycomb-Shaped Material,” IEEE Access, vol. 8, pp. 191090-191099, 2020.

[6] S. Zhang, C. C. Njoku, W. G. Whittow, and J. C. Vardaxoglou, “Novel 3D printed synthetic dielectric substrates”, Microw. Opt. Technol. Lett., vol. 57, no. 10, pp. 2344-2346, 2015.

[7] A. Eid, J. G. D. Hester, J. Costantine, Y. Tawk, A. H. Ramadan, and M. M. Tentzeris, “A Compact Source–Load Agnostic Flexible Rectenna Topology for IoT Devices,” IEEE Trans. Antennas Propag., vol. 68, no. 4, pp. 2621-2629, April 2020.

[8] M. Wagih, A. S. Weddell, and S. Beeby, “Meshed High-Impedance Matching Network-Free Rectenna Optimized for Additive Manufacturing,” IEEE Open J. Antennas Propag., vol. 1, pp. 615-626, 2020.

[9] C. Song et al., “Matching Network Elimination in Broadband Rectennas for High-Efficiency Wireless Power Transfer and Energy Harvesting,” IEEE Trans. Ind. Electron., vol. 64, no. 5, pp. 3950-3961, May 2017.

[10] T. S. Almoneef, “Design of a Rectenna Array Without a Matching Network,” IEEE Access, vol. 8, pp. 109071-109079, 2020.

[11] R. E. Collin, “Limitations of the Thevenin and Norton equivalent circuits for a receiving antenna,” IEEE Antennas Propag. Mag., vol. 45, pp. 119–124, April 2003.